


RESEARCH PAPER

Serelaxin enhances the therapeutic effects of human amnion epithelial cell-derived exosomes in experimental models of lung disease

Simon G. Royce^{1,2} | Krupesh P. Patel¹ | WeiYi Mao¹ | Dandan Zhu³ | Rebecca Lim³ |
 Chrishan S. Samuel^{1,4} 

¹ Cardiovascular Disease Program, Monash Biomedicine Discovery Institute and Department of Pharmacology, Monash University, Clayton, Victoria, Australia

² Department of Medicine, Central Clinical School, Monash University, Clayton, Victoria, Australia

³ The Ritchie Centre, Hudson Institute of Medical Research and Department of Obstetrics and Gynecology, Monash University, Clayton, Victoria, Australia

⁴ Department of Biochemistry and Molecular Biology, University of Melbourne, Parkville, Victoria, Australia

Correspondence

Associate Professor Chrishan S. Samuel,
 Department of Pharmacology, Monash University, Clayton, VIC 3800, Australia.
 Email: chrishan.samuel@monash.edu

Funding information

Monash Innovation Research Funding; National Health and Medical Research Council, Grant/Award Number: GNT1041766; Monash University MBio Postgraduate Discovery Scholarship

Background and Purpose: There is growing interest in stem cell-derived exosomes for their therapeutic and regenerative benefits given their manufacturing and regulatory advantages over cell-based therapies. As existing fibrosis impedes the viability and efficacy of stem cell/exosome-based strategies for treating chronic diseases, here we tested the effects of the anti-fibrotic drug, serelaxin, on the therapeutic efficacy of human amnion epithelial cell (AEC)-derived exosomes in experimental lung disease.

Experimental Approach: Female Balb/c mice were subjected to either the 9.5-week model of ovalbumin and naphthalene (OVA/NA)-induced chronic allergic airway disease (AAD) or 3-week model of bleomycin (BLM)-induced pulmonary fibrosis; then administered increasing concentrations of AEC-exosomes (5 µg or 25µg), with or without serelaxin (0.5mg/kg/day) for 7-days. 1x10⁶ AECs co-administered with serelaxin over the corresponding time-period were included for comparison in both models, as was pirfenidone-treatment of the BLM model. Control groups received saline/corn oil or saline, respectively.

Key Results: Both experimental models presented with significant tissue inflammation, remodelling, fibrosis and airway/lung dysfunction at the time-points studied. While AEC-exosome (5 µg or 25µg)-administration alone demonstrated some benefits in each model, serelaxin was required for AEC-exosomes (25µg) to rapidly normalise chronic AAD-induced airway fibrosis and airway reactivity, and BLM-induced lung inflammation, epithelial damage and subepithelial/basement membrane fibrosis. Combining serelaxin with AEC-exosomes (25µg) also demonstrated broader protection compared to co-administration of serelaxin with 1x10⁶ AECs or pirfenidone.

Conclusions and Implications: Serelaxin enhanced the therapeutic efficacy of AEC-exosomes in treating basement membrane-induced fibrosis and related airway dysfunction.

Abbreviations: AAD, allergic airway disease; ABPAS, Alcian blue periodic acid Schiff; AHR, airway hyperresponsiveness; AI, airway inflammation; AWR, airway remodelling; α-SMA, α-smooth muscle actin; BLM, bleomycin; BM, basement membrane; CO, corn oil; cDyn, dynamic compliance; ECM, extracellular matrix; EXO, exosomes; IHC, immunohistochemistry; IL, interleukin; in, intranasal; MSCs, mesenchymal stem cells; NA, naphthalene; OD, optical density; OVA, ovalbumin; PBS, phosphate-buffered saline; H2, human gene-2; NA, naphthalene; OVA, ovalbumin; RLX, recombinant human relaxin drug/serelaxin; RXFP1, relaxin family peptide receptor 1; SAL, saline; TGF-β1, transforming growth factor-β1.

Simon G. Royce, Krupesh P. Patel and WeiYi Mao contributed equally to this work.

1 | INTRODUCTION

Fibrosis (scar tissue accumulation) results from a failed wound healing response to tissue injury, where extracellular matrix (ECM) synthesis is ongoing and further exacerbates tissue damage in a self-perpetuating cycle (Eming, Wynn, & Martin, 2017; Wynn & Ramalingam, 2012). This depends largely on the activation of ECM-producing myofibroblasts (activated fibroblasts), which in turn are influenced by several mediators, particularly **transforming growth factor (TGF)- β 1** (Royce, Patel, & Samuel, 2014). Additionally, newly-secreted ECM components can be remodelled and reorganised by several proteases (Afratis, Selman, Pardo, & Sagi, 2018). An imbalance of ECM and in particular, collagen synthesis over degradation accelerates fibrosis progression, which in turn leads to significant tissue dysfunction and ultimately, organ failure.

The rate and severity of fibrosis can also affect the efficacy of various therapeutic strategies aimed at stopping or at least slowing its progression. This is particularly evident for stem cell-based therapies, where the fibrosis associated with chronic organ disease has been shown to hinder stem cell survival and accessibility to sites of damage (Eun et al., 2011; Lu, Zhang, Ramires, & Sun, 2004). To overcome these limitations, we recently utilised a bimodal ablation of fibrosis associated with obstructed nephropathy (Huuskens et al., 2015) or chronic allergic airway disease (AAD) (Royce et al., 2015, 2016) with an anti-fibrotic, serelaxin, to create a more compatible environment that would enhance the therapeutic viability and function of exogenously administered human bone marrow-derived mesenchymal stem cells (MSCs) or human amnion epithelial cells (AECs). Serelaxin (RLX) is the recombinantly-produced form of the major stored and circulating hormone (Samuel et al., 2017; Sarwar, Du, Dschietzig, & Summers, 2017) and mediates its actions via its cognate G protein-coupled receptor, relaxin family peptide receptor 1 (RXFP1) (Bathgate et al., 2013). Serelaxin augmented the therapeutic potential of RXFP1-expressing MSCs (Huuskens et al., 2015; Royce et al., 2015, 2016) or AECs (Royce et al., 2016) by not only creating an improved environment in which these stem cells could survive and function, but by also directly increasing their ability to proliferate and migrate.

AECs contain a number of properties which make them suitable candidates for treating fibrosis-related disorders. They are non-immunogenic (Akle, Adinolfi, Welsh, Leibowitz, & McColl, 1981), can be easily and ethically isolated by non-invasive procedures from the amnion sac of the mature placenta (Miki, Lehmann, Cai, Stolz, & Strom, 2005), can differentiate into all three germ layers (Miki et al., 2005) and demonstrate anti-inflammatory, anti-fibrotic and tissue-reparative functions (Moodley et al., 2010). However, as like other stem cells, it is possible that AECs mediate their therapeutic/reparative effects through paracrine factors or vesicles known as exosomes (EXO), which contain secreted bioactive substances such as proteins, mRNAs and microRNAs (Tan et al., 2018). EXO mediate regenerative outcomes in injury and disease that recapitulate observed bioactivity of stem cell populations (Basu & Ludlow, 2016). Encapsulation of the active biological ingredients of regeneration within non-living exosome carriers

What is already known

- Fibrosis impairs the viability and efficacy of exogenously administered stem cells in chronic disease settings.
- Stem cell-derived exosomes offer several manufacturing and regulatory advantages as therapies over their parental cells.

What this study adds

- The therapeutic effects of stem cell-derived exosomes can also be impaired by fibrosis.
- The anti-fibrotic drug serelaxin enhances the therapeutic efficacy of human amnion epithelial cell-derived exosomes.

What is the clinical significance

- The therapeutic benefits of amnion epithelial cell-derived exosomes can be augmented by reducing airway/lung fibrosis.
- Amnion epithelial cell-exosomes offer broader tissue protection over cell therapy when fibrosis is reduced.

may offer process, manufacturing and regulatory advantages over stem cell-based therapies; allowing for the transfer of proteins and nucleic acids across cellular boundaries. Furthermore, AEC-derived EXO offer the therapeutic potential of several million AECs.

In this study, we determined how effective increasing concentrations of AEC-derived EXO (EXO; 5 μ g vs. 25 μ g) were in reversing ovalbumin and naphthalene (OVA/NA)-induced chronic AAD- and bleomycin (BLM)-induced interstitial and basement membrane (BM)/subepithelial lung fibrosis. More importantly, we determined if the anti-fibrotic and organ-protective effects of RLX (Samuel et al., 2017; Sarwar et al., 2017) would enhance the therapeutic effects of EXO in each model studied.

2 | METHODS

2.1 | Animals

Seven-to-eight week-old female Balb/c wild-type mice (RRID: IMSR_JAX:000651; provided by Monash University Animal Services, Clayton, Victoria, Australia) were allowed to acclimatize for at least 4-to-5 days prior to experimentation and were maintained on a 12 h light:12 h dark cycle with free access to standard rodent chow (Barastoc Stockfeeds, Pakenham, Victoria, Australia) and water. Female Balb/c wild-type mice have been shown to be more prone to a Th2 response and undergo higher airway reactivity (in response to allergens) compared with their male counterparts and other commonly used murine strains (Kumar, Herbert, & Foster, 2008). All experiments

described below were approved by Monash University's Animal Ethics Committee, which adheres to the Australian Code of Practice for the Care and Use of Laboratory Animals for Scientific Purposes. Power calculations were performed to ensure that adequate group sizes were used for the studies detailed below; where it was determined that with a 20% standard deviation, we would be 80% powered to detect a 25-27% effect with $n=7-8$ animals per group. Animal studies are reported in compliance with the ARRIVE guidelines (Kilkenny, Browne, Cuthill, Emerson, & Altman, 2010) and with the recommendations made by the *British Journal of Pharmacology*.

2.2 | Induction and treatment of chronic AAD incorporating epithelial damage

Female Balb/c mice ($n=8$ /group) sensitized with two i.p. injections of 10 μg grade V chicken egg OVA (Sigma-Aldrich, St Louis, MO, USA) and 1 mg aluminum potassium sulfate adjuvant (alum; AJAX Chemicals, Kotara, NSW, Australia) in 0.5 ml of saline on Days 0 and day 14. They were then subjected to nebulization (inhalation of an aerosol) with 2.5% (w/v) OVA for 30 min, three times a week, between Days 21 and 63, using an ultrasonic nebulizer (Omron NE-U07; Omron, Kyoto, Japan). The mice then received a single i.p. injection of the Clara cell-specific cytotoxin, naphthalene (NA; 200 mg/kg body weight; Sigma-Aldrich) on Day-64 (1-day after the last OVA nebulization period) and left for a further three days. A separate subgroup of mice ($n=8$) subjected to i.p. injections of saline SAL on Days-0 and -14, nebulized saline SAL instead of OVA between Days-21 and 63, and an i.p. injection of corn oil (CO; the vehicle for NA) were included as a control group.

2.3 | Induction of bleomycin (BLM)-induced pulmonary fibrosis

Female Balb/c mice ($n=7$ /group) were intranasally (i.n.) administered bleomycin sulfate (Hospira Healthcare Corp., Melbourne, Victoria, Australia; RRID:SCR_003985) on Days-0 and -7 (0.15mg in 50 μl of saline SAL on each day) (Moodley et al., 2010), then left for a further two weeks for lung inflammation and fibrosis to develop. Female Balb/c mice were used for consistency (with that used in the chronic AAD model), and although they are more resistant to BLM-induced injury compared to other strains of mice (Moeller, Ask, Warburton, Gaudie, & Kolb, 2008), direct double-hit administration of BLM to the lungs of these mice was expected to provoke significant lung inflammation, remodelling and fibrosis in these animals. Control mice ($n=7$) were i.n. administered 50 μl of saline SAL on Days-0 and -7, and maintained until Day 21.

2.4 | Isolation and characterisation of AEC-derived exosomes (EXO)

AECs were isolated from placentae of women undergoing elective caesarean section (at 38-42 weeks of gestation) in accordance with

guidelines and approval from the Monash Health Human Research Ethics Committee. AECs were isolated from several pooled amnions and reconstituted overnight once thawed from being stored in liquid nitrogen, as described before (Murphy et al., 2010, 2014). 1×10^6 AECs were then resuspended in saline SAL for therapeutic administration as detailed below. EXO were isolated from several pooled amnions and characterised as described previously (Tan et al., 2018). EXO were then dissolved in saline SAL for therapeutic administration as detailed below. Proteomic pathway clustering analysis including proteins significantly enriched by EXO and RNA sequencing analysis of EXO were recently reported (Tan et al., 2018).

2.5 | Treatment groups

On Day-67 of the chronic AAD model (3 days post-NA administration) or Day-21 of the BLM model, sub-groups of mice received either i) 5 μg EXO alone (half the dose evaluated previously (Tan et al., 2018)); ii) 5 μg EXO+RLX (0.5mg/kg/day; a dose that has previously been used to demonstrate its anti-fibrotic efficacy) (Huuskens et al., 2015; Royce et al., 2015, 2016); iii) 25 μg EXO alone (a 5-fold increase of the 5 μg dose; to determine the dose-dependent effects of EXO); iv) 25 μg EXO+ RLX; or v) 1×10^6 AECs+ RLX (Royce et al., 2016). EXO or AECs were i.n.-instilled into mice, while RLX was subcutaneously administered via osmotic mini-pumps (Model 1007D, Alzet, Cupertino, CA, USA). All treatments were maintained for 7-day period. As the effects of RLX alone were previously evaluated in the chronic AAD model over the same time-period (Patel, Giraud, Samuel, & Royce, 2016), the data previously obtained (from $n=8$ mice) has been included to provide comparisons to the combination treatment groups evaluated in the current study. Additionally, the effects of vi) the TGF- β 1 blocker, Pirfenidone (100mg/kg/day; administered twice daily by oral gavage over a 7-day period) (Oku et al., 2008) were also evaluated in the BLM model.

2.6 | Airway and lung function evaluation

On Day-75 of the chronic AAD model and Day-29 of the BLM model (24 hours after the 7 day-treatment period in each case), mice were evaluated by plethysmography for changes in airway hyperresponsiveness (AHR) (Royce et al., 2015, 2016) or dynamic lung compliance (Patel et al., 2016), respectively; in response to increasing concentrations of -induced airway bronchoconstriction. Mice were briefly anesthetized with an i.p. injection of ketamine (100 mg/kg body weight) and xylazine (20 mg/kg body weight), tracheostomized and cannulated. Increasing doses of methacholine (0-50mg/ml) were nebulized and AHR was measured (Biosystem XA version 2.7.9, Buxco Electronics, Troy, NY, USA) for 2 min after each dose. For the BLM model, results were expressed as the percentage change in dynamic compliance after each dose of methacholine from baseline compliance.

2.7 | Tissue collection

Once airway reactivity measurements were completed, mice were culled with an overdose of anesthetic containing ketamine and xylazine, before their lung tissue isolated. The lungs of each animal were then divided along the transverse plane, resulting in four separate lobes. In each case, the largest lung lobe was fixed in 10% neutral buffered formalin overnight and processed to be cut and embedded in paraffin wax. The remaining lobes were separately snap-frozen in liquid nitrogen and eventually stored at -80 °C for various other assays.

2.8 | Tissue histopathology and immunohistochemistry

The antibody-based procedures used in this study comply with the recommendations made by the *British Journal of Pharmacology*. Serial paraffin-embedded lung sections (3 µm thickness) were placed on charged Mikro Glass slides (Grale Scientific, Ringwood, Victoria, Australia) and subjected to Mayer's haematoxylin and eosin (Amber Scientific, Midvale, Western Australia, Australia; H&E), Masson's trichrome, or Alcian blue periodic acid Schiff (ABPAS) staining for assessment of airway/lung inflammation, epithelial thickness and subepithelial collagen deposition, and goblet cell metaplasia respectively (Royce et al., 2015, 2016). Separate slides were immunohistochemically stained for airway/lung TGF-β1 (using a polyclonal antibody; sc-146; Santa Cruz Biotechnology, Santa Cruz, CA, USA; 1:1,000 dilution), airway/lung α-smooth muscle actin (a marker of myofibroblast differentiation; using a monoclonal antibody; M0851; DAKO Antibodies, Glostrup, Denmark; 1:200 dilution), or airway/lung **thymic stromal lymphopoietin (TSLP)**; a marker of epithelial damage; using a polyclonal antibody; ABT330; EMD Millipore Corp'. Temecula, CA, USA; 1:1,000 dilution). Detection of antibody staining was completed using the DAKO EnVision anti-mouse (K4001) or anti-rabbit (K4003; RRID:AB_2630375) kits, respectively, and 3,3-diaminobenzidine (Sigma-Aldrich), where sections were counterstained with haematoxylin. Images of five bronchi (measuring 150–350-µm luminal diameter) per section were obtained and quantified by morphometry, as described below. All slides were then scanned at the maximum magnification available (40×) and stored as digital high resolution images on a local server associated with the instrument. Digital slides were viewed and morphometrically analysed with the Aperio ImageScope v.12.1.0.5029 software (Leica Biosystems, Nussloch, Germany)

2.9 | Morphometric analysis

Representative photomicrographs from H&E-, Masson's trichrome-, and ABPAS-stained slides, as well as immunohistochemically stained slides, were captured from scanned images using ScanScope AT Turbo (Aperio, CA, USA). Five stained airways were randomly selected from across the tissue sample. Histological grading of inflammation severity

from 0 to 4 was assigned to every slide, as described previously (Royce, Moodley, & Samuel, 2014; 0 = no detectable inflammation; 1 = occasional inflammatory cell aggregates, pooled size <0.1 mm²; 2 = some inflammatory cell aggregates, pooled size ~0.2 mm²; 3 = widespread inflammatory cell aggregates, pooled size ~0.3 mm²; and 4 = widespread and massive inflammatory cell aggregates, pooled size ~0.6 mm²), and was performed blinded by the investigator. High-power H&E-stained slides (from the BLM model) were also used to evaluate neutrophil and macrophage counts from five fields per section, respectively, as identified previously (Molnar & Gain, 2012) and expressed as the relative cell counts to that in the untreated control groups, which was expressed as 1 in each case. Neutrophils (polymorphonuclear leukocytes) were identified by their segmented multi-lobulated nuclei, and macrophages were identified by their cytological features of larger size and paler more spherical nucleus and larger cytoplasm. Masson's trichrome-stained slides were analysed by measuring the thickness of the epithelial and subepithelial layers and expressing values as µm²·mm⁻¹ BM length. ABPAS-stained slides were analysed by counting the number of stained goblet cells, which were expressed as the number of goblet cells per 100-µm BM length. α-Smooth muscle actin- and TSLP- positively stained cells located within the subepithelial or interstitial and epithelial regions, respectively, of the airway were counted and expressed as number of positively stained cells per 100-µm BM length. Interstitial TGF-β1 staining was quantified by measuring the levels of strong positively stained areas within the epithelial and interstitial regions, respectively; and expressing the data as the % epithelial TGF-β1 staining/field or relative % interstitial TGF-β1 staining/field compared to that in the untreated control group, which was expressed as 1.

2.10 | Hydroxyproline assay

The second largest lung lobe from each mouse was processed as described before (Royce et al., 2015, 2016) for the measurement of hydroxyproline content, which was determined from a standard curve of purified trans-4-hydroxy-L-proline (Sigma-Aldrich). Hydroxyproline values were multiplied by a factor of 6.94 (based on hydroxyproline representing ~14.4% of the amino-acid composition of collagen in most mammalian tissues; Gallop & Paz, 1975) to extrapolate total collagen content, which in turn was divided by the dry weight of each corresponding tissue to yield percent collagen concentration.

2.11 | Data and statistical analysis

The data and statistical analysis in this study comply with the recommendations of the *British Journal of Pharmacology* on experimental design and analysis in pharmacology. All statistical analyses were performed using GraphPad Prism v7.0 (GraphPad Software Inc., CA, USA; RRID:SCR_002798) and expressed as the mean ± SEM. AHR results were analysed by a two-way ANOVA with Bonferroni post hoc test. The remaining data were analysed via a one-way ANOVA with

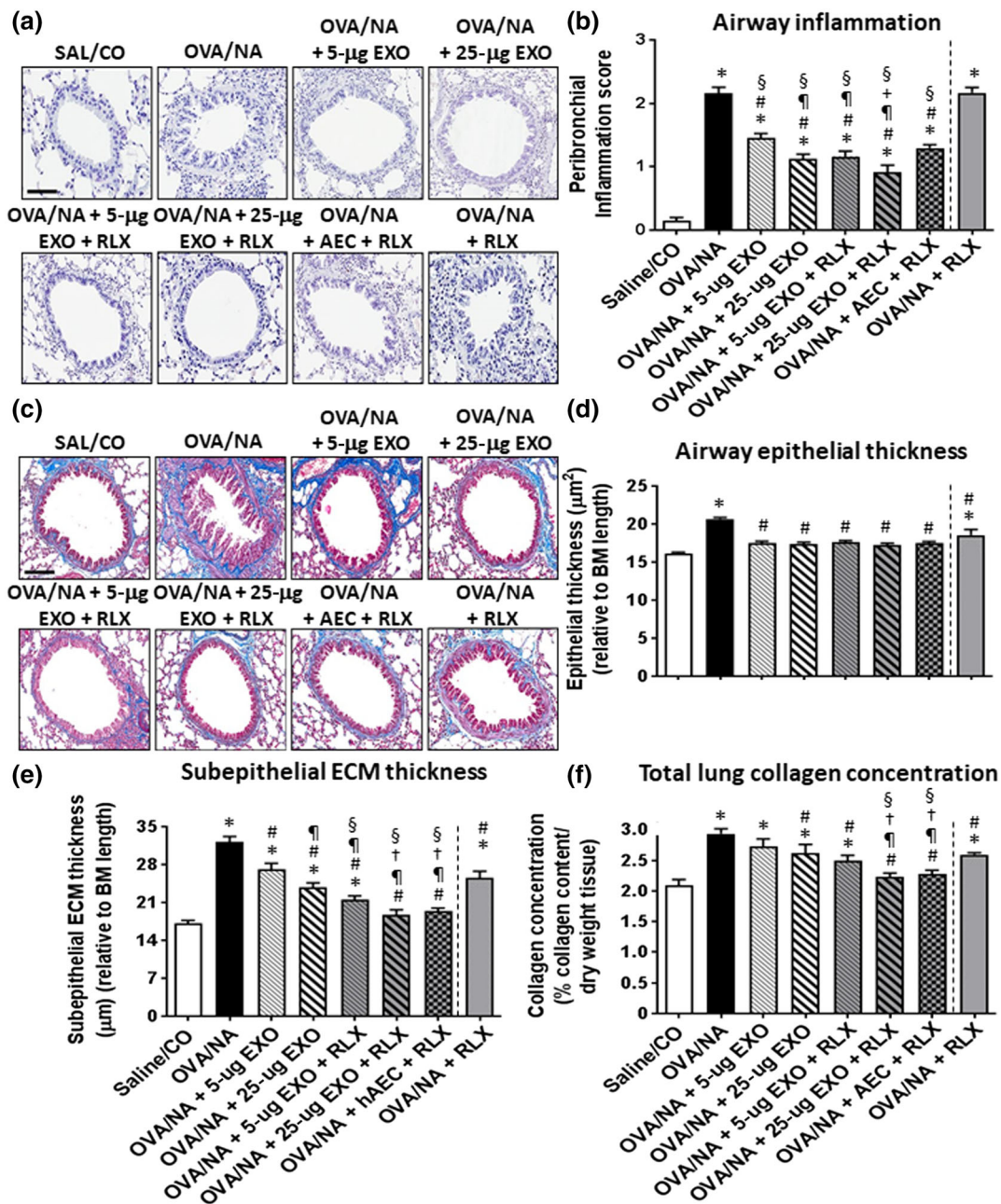


FIGURE 1 The effects of exosomes (EXO) on chronic AAD-induced airway inflammation and fibrosis in the absence or presence of serelaxin. Representative images of H&E-stained lung sections from mice subjected to OVA/ naphthalene (OVA/NA)-induced chronic AAD and the various treatment strategies investigated (a) demonstrate the extent of inflammatory cell infiltration within the bronchial wall. Scale bar = 50 μm . Representative images of Masson's trichrome-stained lung sections from mice subjected to OVA/ naphthalene-induced chronic AAD and the various treatment strategies investigated (c) demonstrate the extent of airway epithelial thickening and subepithelial ECM/collagen deposition around the airways. Scale bar = 50 μm . In each case, the effects of serelaxin (RLX) alone (previously evaluated in this model over the same time period; Patel et al., 2016) have been included to provide comparisons to the combination treatment groups evaluated in the current study. Also shown is the OVA-NA-induced peribronchial inflammation score, as means \pm SEM (b) from five airways per mouse—where sections were scored based on the number and distribution of inflammatory cell aggregates on a scale of 0 (no visible inflammation) to 4 (severe inflammation); airway epithelial thickness (d); subepithelial ECM thickness (e); and total collagen concentration (f) from five airways per mouse; $n = 8$ animals per group. * $P < 0.05$, significantly different from the uninjured control group (SAL/CO); # $P < 0.05$, significantly different from the OVA/NA-treated group; † $P < 0.05$, significantly different from the OVA/NA + 5- μg EXO group; ‡ $P < 0.05$, significantly different from the OVA/NA + 25- μg EXO-treated group; § $P < 0.05$ significantly different from the OVA/NA + AEC + RLX-treated group; ¶ $P < 0.05$ significantly different from the OVA/NA + RLX-treated group. EXO, exosomes

Neuman-Keuls post hoc test for multiple comparisons between groups. In each case, differences between means were significant when $P < 0.05$.

2.12 | Materials

Bleomycin was supplied by Hospira Healthcare Corp., (Melbourne, Victoria, Australia); methacholine by Sigma Aldrich (St Louis, MO, USA); pirfenidone by In Vitro Technologies, (Noble Park, Victoria, Australia) and serelaxin by Corthera Inc (San Mateo, CA, USA)

2.13 | Nomenclature of targets and ligands

Key protein targets and ligands in this article are hyperlinked to corresponding entries in <http://www.guidetopharmacology.org>, the common portal for data from the IUPHAR/BPS Guide to PHARMACOLOGY (Harding et al., 2018), and are permanently archived in

the Concise Guide to PHARMACOLOGY 2017/18 (Alexander, Christopoulos et al., 2017; Alexander, Fabbro et al., 2017a, b).

3 | RESULTS

3.1 | Serelaxin may augment the anti-inflammatory effects of AEC-exosomes

At the designated time point of each model studied, OVA/NA-induced peribronchial airway inflammation (Figure 1a,b) and BLM-induced interstitial lung inflammation (Figure 2a-d) were significantly increased by ~2.5- to 14-fold, compared to corresponding measurements obtained from uninjured, control groups. In the BLM model, the elevated lung inflammation was associated with significantly increased neutrophil (Figure 2c) and macrophage (Figure 2d) infiltration, in the absence of any changes in animal body weight or mortality.

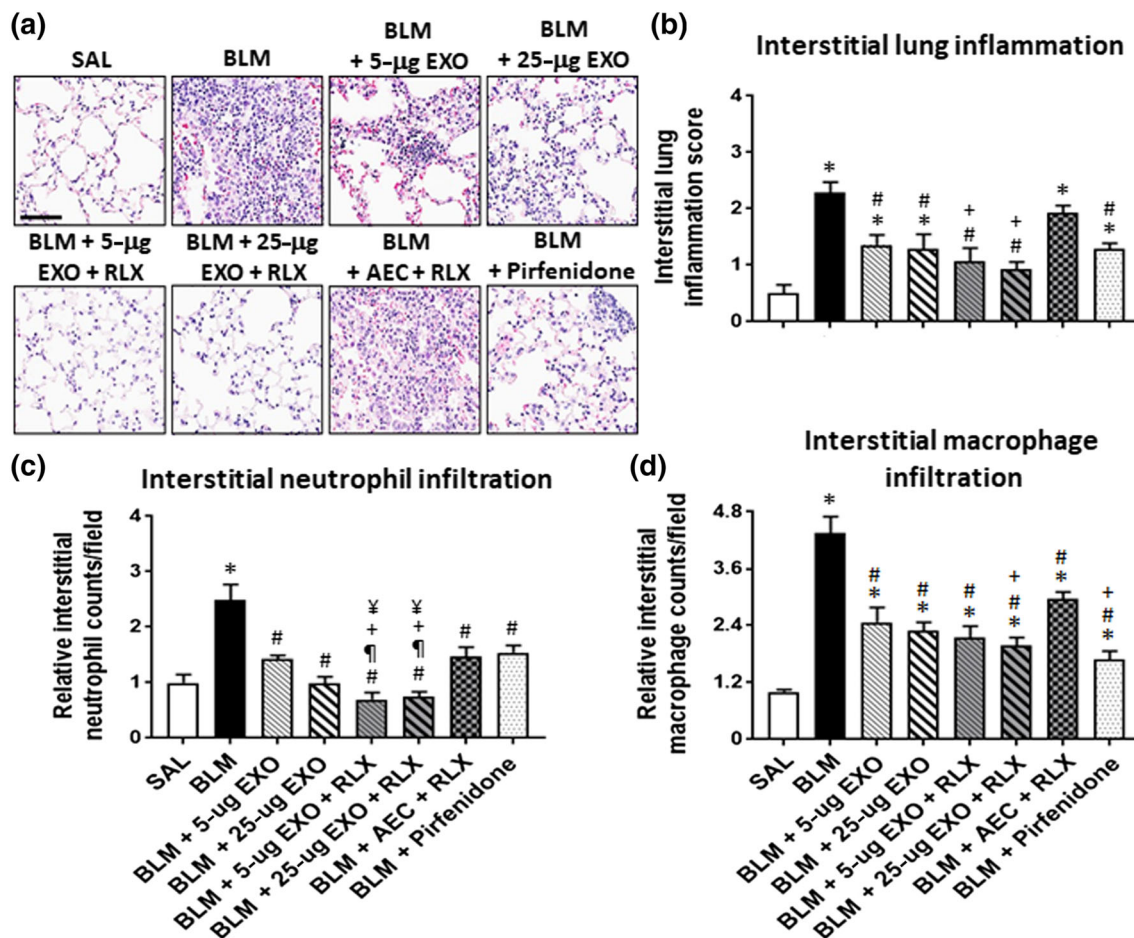


FIGURE 2 The effects of exosomes (EXO) on BLM-induced lung inflammation, with or without serelaxin (RLX). Representative images of H&E-stained lung sections from mice subjected to BLM-induced pulmonary fibrosis and the various treatment strategies investigated (a) demonstrate the extent of interstitial lung inflammation. Scale bar = 80 µm. Also shown is the mean ± SEM BLM-induced interstitial inflammation score (b), neutrophil counts (c), and macrophage counts (d) from 5 to 6 fields per mouse section; $n = 7$ animals per group. * $P < 0.05$, significantly different from the control group (SAL); # $P < 0.05$, significantly different from the BLM-treated injured group; † $P < 0.05$, significantly different from the BLM + 5-µg EXO-treated group; ‡ $P < 0.05$, significantly different from the BLM + 25-µg EXO-treated group; § $P < 0.05$, significantly different from the BLM + RLX-treated group

Exosomes alone (5 or 25 μg) were able to partly (by ~35–56%), but not fully, reduce the extent of the general inflammation measured by 7-day post-administration. While the anti-inflammatory effects of exosomes were dose-dependent in the chronic AAD model (Figure 1a,b) with 25- μg exosomes reducing airway inflammation to a greater extent than 5- μg exosomes, the effects of exosomes against BLM-induced interstitial lung inflammation were not dose-dependent (Figure 2a–d).

Noticeably, some anti-inflammatory effects of 5- μg exosomes were augmented in the presence of serelaxin. Although serelaxin alone did not affect OVA/NA-induced airway inflammation (Figure 1a,b), it did enhance the anti-inflammatory (Figure 1b) and neutrophil-inhibitory (Figure 2c) effects of 5- μg exosomes in the chronic AAD and BLM models respectively. Combining serelaxin with 25- μg exosomes also appeared to optimally reduce OVA/NA-induced airway inflammation (Figure 1b) and BLM-induced interstitial lung inflammation (Figure 2b) by ~60–100% and induce a trend towards reducing these parameters over the effects of 25- μg exosomes alone, although the combined effects of serelaxin and 25- μg exosomes were not statistically different to that of 25- μg exosomes alone. Of note, co-administration of 25- μg exosomes and serelaxin reduced BLM-

induced inflammation to levels that were no longer different from that in SAL-treated controls. Furthermore, the combined effects of 25- μg exosomes and serelaxin significantly reduced OVA/NA-induced airway inflammation (Figure 1b) and BLM-induced interstitial lung inflammation (Figure 2b), neutrophil infiltration (Figure 2c), and macrophage infiltration (Figure 2d) to a significantly greater extent than 1×10^6 AECs co-administered with serelaxin. Additionally, the combined effects of 25- μg exosomes and serelaxin significantly reduced BLM-induced neutrophil infiltration to a significantly greater extent than pirfenidone (Figure 2c), which only partially reduced overall lung inflammation by 55–60% (Figure 2b), but had similar effects to that of pirfenidone in reducing macrophage infiltration (Figure 2d).

3.2 | Serelaxin enhances the anti-fibrotic effects of exosomes

OVA/NA-induced airway epithelial thickness (Figure 1c,d), subepithelial ECM thickness (Figure 1e) and total lung collagen concentration (Figure 1f); and BLM-induced interstitial lung fibrosis (Figure 3a,b) and subepithelial ECM thickness (Figure 3c,d) were all

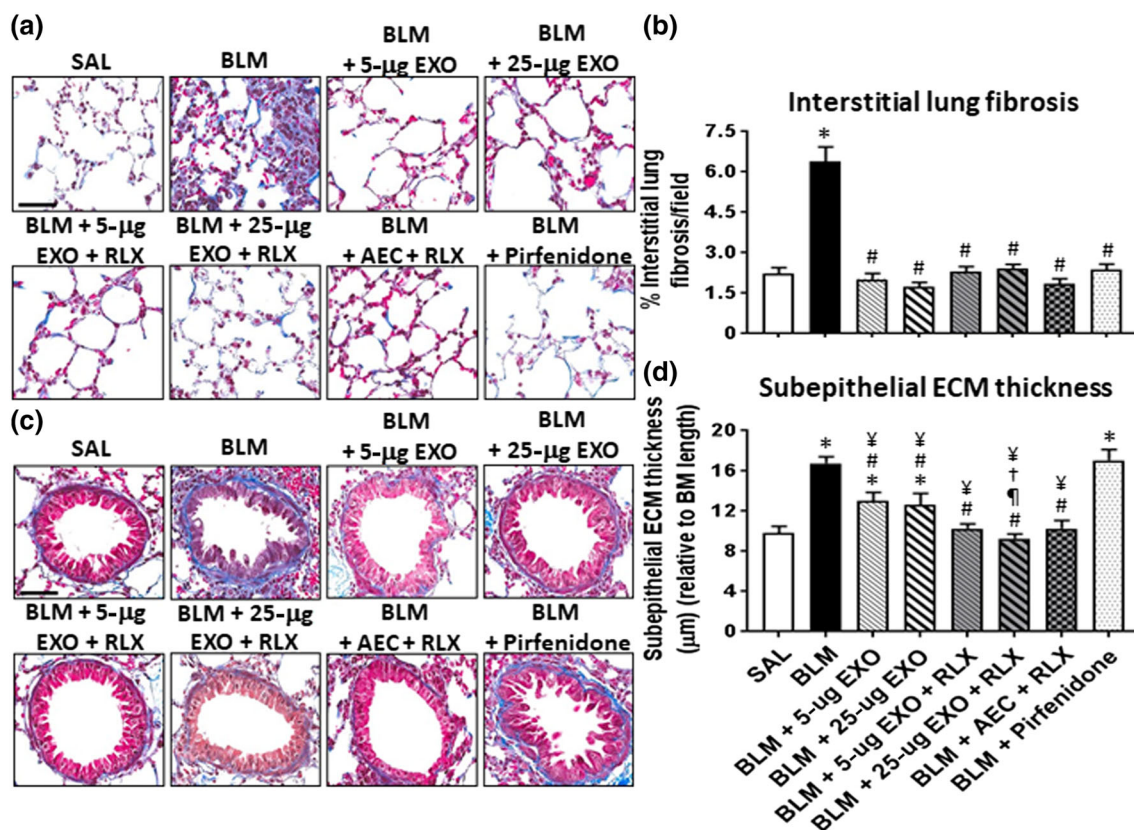


FIGURE 3 The effects of exosomes (EXO) on BLM-induced lung fibrosis in the absence or presence of serelaxin. Representative images of Masson's trichrome-stained lung sections from mice subjected to BLM-induced pulmonary fibrosis and the various treatment investigated demonstrate the extent of interstitial (a) and subepithelial ECM/collagen deposition around the airways (c). Scale bar = 50 μm in each case. Also shown is the mean \pm SEM BLM-induced interstitial (b) and subepithelial (d) ECM/collagen deposition from 5 to 6 fields per section; $n = 7$ animals per group. * $P < 0.05$, significantly different from the control group (SAL); # $P < 0.05$, significantly different from the BLM-treated injured group; † $P < 0.05$, significantly different from the BLM + 5- μg EXO-treated group; ‡ $P < 0.05$, significantly different from the BLM + 25- μg EXO-treated group; § $P < 0.05$, significantly different from the BLM + Pirfenidone-treated group

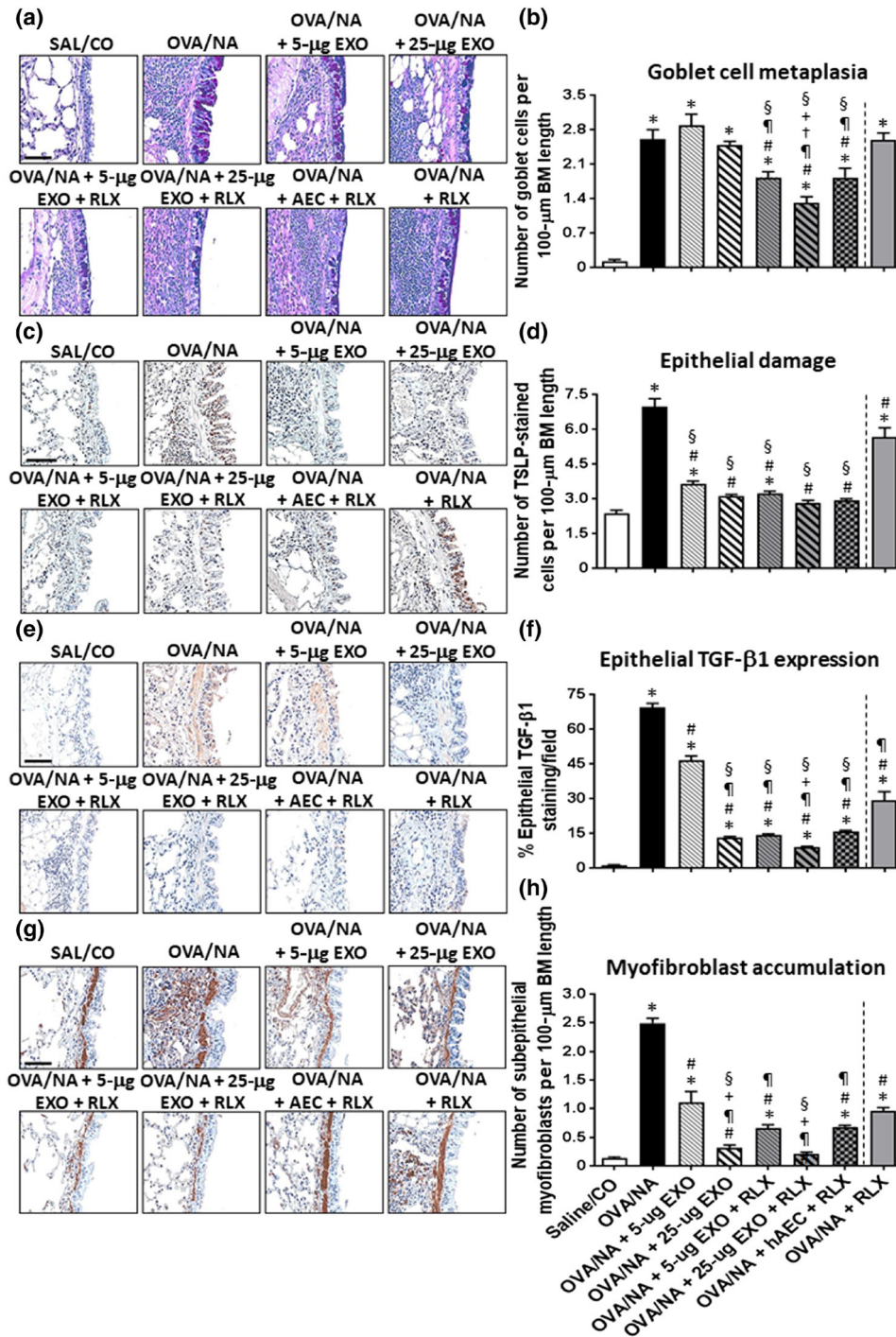


FIGURE 4 The effects of exosomes (EXO) on chronic AAD-induced airway remodelling in the absence or presence of serelaxin (RLX). Representative images of ABPAS-stained lung sections from mice subjected to OVA/NA-induced chronic AAD and the various treatment investigated (a) demonstrate the extent of goblet cell metaplasia within the airways. Scale bar = 100 μ m. Representative images of immunohistochemically stained lung sections from mice subjected to OVA/NA-induced chronic AAD and the various treatment investigated show the extent of TSLP-associated epithelial damage (c); epithelial TGF- β 1 expression (e); and subepithelial myofibroblast accumulation (g). Scale bar = 50 μ m (c, e, g). In each case, the effects of serelaxin alone (previously evaluated in this model over the same time period; Patel et al., 2016) have been included to provide comparisons to the combination treatment groups evaluated in the current study. Also shown is the mean \pm SEM number of goblet cells per 100- μ m BM length, as mean \pm SEM, induced by OVA/NA (b); number of TSLP-stained cells per 100- μ m BM length (d); % epithelial TGF- β 1 expression levels per field (f); and number of subepithelial myofibroblasts per 100- μ m BM length (h) from five airways per mouse; $n = 8$ animals per group. * $P < 0.05$, significantly different from the control group (SAL/CO); # $P < 0.05$, significantly different from the OVA/NA group; $\dagger P < 0.05$, significantly different from the OVA/NA + 5- μ g EXO-treated group; $\ddagger P < 0.05$, significantly different from the OVA/NA + 25- μ g EXO-treated group; $\S P < 0.05$, significantly different from the OVA/NA + AEC + RLX-treated group; $\P P < 0.05$, significantly different from the OVA/NA + RLX-treated group

significantly increased by ~0.3- to 1.85-fold at the time points measured. While exosomes alone (5 or 25 μg) was able to normalize chronic AAD-induced airway epithelial thickness (Figure 1d) and BLM-induced interstitial lung fibrosis (Figure 3b) by 7 days post-administration, they only partly reduced (by ~25–60%) OVA/NA- (Figure 1e) and BLM-induced (Figure 3d) subepithelial ECM thickness and OVA/NA-induced total lung collagen concentration (Figure 1f) over the same time period. Once again, concentration-dependent effects of exosomes were observed in the chronic AAD model but not in the BLM model.

Strikingly, the combined effects of serelaxin and 25- μg exosomes normalized OVA/NA-induced subepithelial ECM thickness (Figure 1e), total lung collagen concentration (Figure 1f), and BLM-induced subepithelial ECM thickness (Figure 3d), suggesting that this combination strategy offered broader anti-fibrotic effects over that of exosomes alone. Combining serelaxin with 1×10^6 AECs offered equivalent anti-fibrotic effects to that of combining serelaxin and 25- μg exosomes against airway/lung fibrosis (Figure 4c,d,f,h). Additionally, while pirfenidone offered similar protection, to the combined effects of serelaxin and 25- μg exosomes, against BLM-induced interstitial lung fibrosis (Figure 3b), it did not demonstrate any effects against BLM-induced subepithelial ECM thickness/fibrosis (Figure 3d).

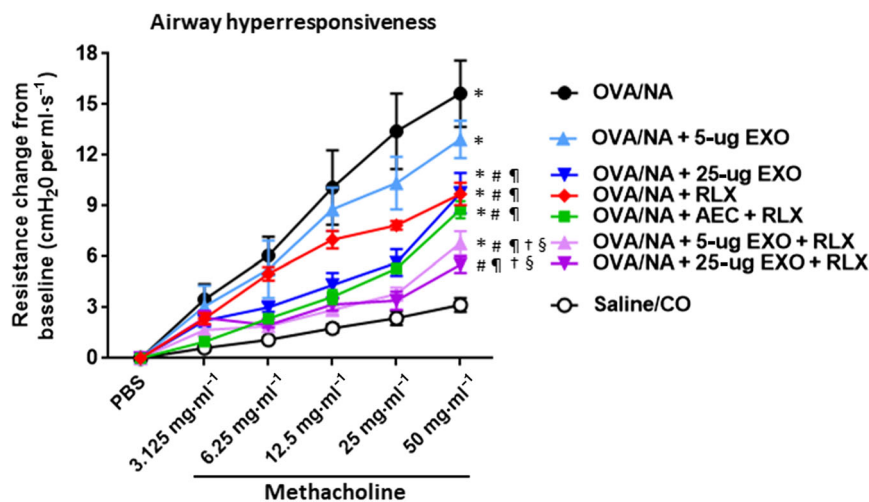
3.3 | Serelaxin augments the anti-remodelling effects of exosomes

Exosomes alone (at 5 or 25 μg) did not affect OVA/NA-induced goblet cell metaplasia (Figure 4a,b), but dose-dependently and partly reduced airway TSLP-associated epithelial damage (Figure 4c,d), epithelial TGF- β 1 expression (Figure 4e,f), and subepithelial myofibroblast accumulation (Figure 4g,h) in the setting of chronic AAD. Additionally, 25- μg exosomes alone reduced airway epithelial TGF- β 1 expression

(by ~80%; Figure 5f) and normalized airway epithelial damage (Figure 5d) and subepithelial myofibroblast accumulation (Figure 5f); 25- μg exosomes, but not 5- μg exosomes, also partly (by ~26%) reduced BLM-induced epithelial damage (Figure 6a,b); while neither dose of exosomes affected BLM-induced interstitial TGF- β 1 expression levels (Figure 6c,d). On the other hand, both doses of exosomes reduced BLM-induced myofibroblast accumulation, by 30–38% (Figure 6e,f).

The presence of serelaxin was able to augment the ability of 5- μg exosomes to reduce chronic AAD-induced goblet cell metaplasia (by ~32%; Figure 4b), epithelial TGF- β 1 expression (by ~80%; Figure 4f), and subepithelial myofibroblast differentiation (by ~77%; Figure 4h) and reduce BLM-induced lung epithelial damage (by ~27%; Figure 6b) and interstitial TGF- β 1 expression (by 70–75%; Figure 6d) over as little as a 7-day treatment period. Combining serelaxin with 25- μg exosomes further reduced chronic AAD-induced goblet cell metaplasia (by ~52%; Figure 4b) and BLM-induced epithelial damage and interstitial TGF- β 1 expression (by 70–75%; Figure 6b,d) as well as interstitial myofibroblast accumulation (by ~60%; Figure 6f). Notably, the combined effects of serelaxin and 25- μg exosomes also normalized chronic AAD- (Figure 4d) and BLM-induced (Figure 6d) airway/lung epithelial damage but otherwise maintained the anti-remodelling effects of 25- μg exosomes on airway epithelial TGF- β 1 expression (Figure 4f) and myofibroblast accumulation (Figure 4h). Combining serelaxin with 25- μg exosomes had a greater effect in reducing the chronic AAD-induced remodelling parameters measured compared to the effects of serelaxin alone or the combined effects of serelaxin and 1×10^6 AECs (Figure 4); and had a greater ability to reduce BLM-induced lung remodelling (Figure 6) compared to the combined effects of serelaxin and 1×10^6 AECs or pirfenidone. Interestingly, our data suggested that pirfenidone most likely exerted its effects post-BLM-induced injury by inhibiting TGF- β 1 signal transduction and activity rather than altering TGF- β 1 expression levels (Figure 6d) per se.

FIGURE 5 The effects of exosomes (EXO) on chronic AAD-induced airway reactivity in the absence or presence of serelaxin (RLX). Shown is the SAL/CO versus OVA/NA-induced airway resistance change from baseline ($\text{cmH}_2\text{O ml}^{-1}\cdot\text{s}^{-1}$) and from each of the treatment groups investigated against OVA/NA-induced chronic AAD, in response to increasing concentrations of the bronchoconstrictor, methacholine; mean \pm SEM from $n = 8$ mice per group. * $P < 0.05$, significantly different from the control group (SAL/CO); # $P < 0.05$, significantly different from the OVA/NA group; † $P < 0.05$, significantly different from the OVA/NA + 5- μg EXO-treated group; ‡ $P < 0.05$, significantly different from the OVA/NA + 25- μg EXO-treated group; § $P < 0.05$ significantly different from the OVA/NA + RLX-treated group



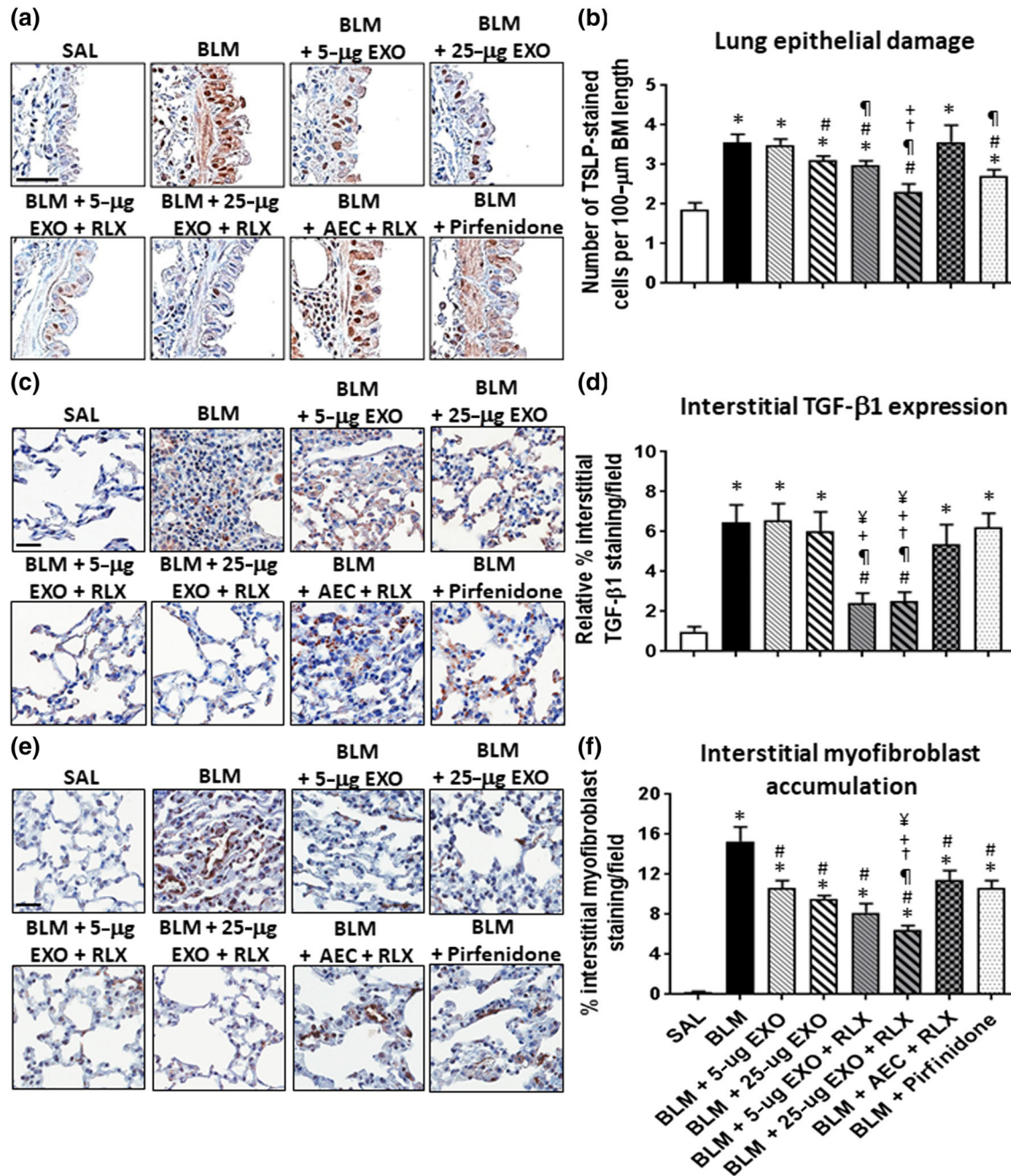


FIGURE 6 The effects of exosomes on BLM-induced lung remodelling in the absence or presence of serelaxin (RLX). Representative images of TSLP (a), TGF-β1 (c), and α-SMA (e)-stained lung sections from mice subjected to BLM-induced pulmonary fibrosis and the various treatment investigated demonstrate the extent of airway epithelial damage (a), interstitial TGF-β1 expression levels (c), and interstitial myofibroblast accumulation (e) within the lung. Scale bar = 50 µm in each case. Also shown is the mean ± SEM BLM-induced number of TSLP-stained cells per 100-µm BM length (b); relative interstitial TGF-β1 staining/field (d); and % interstitial myofibroblast staining/field (f) from 5 to 6 fields/mouse section; $n = 7$ animals/group. * $P < 0.05$ versus SAL-treated uninjured control group; # $P < 0.05$ versus BLM-treated injured group; ¶ $P < 0.05$ versus BLM + 5-µg EXO-treated group; † $P < 0.05$ versus BLM + 25-µg EXO-treated group; ‡ $P < 0.05$ versus BLM + AEC + RLX-treated group; ¥ $P < 0.05$ versus BLM + Pirfenidone-treated group

3.4 | Serelaxin augments the ability of exosomes to reduce airway reactivity

Plethysmography was used to measure OVA/NA-induced AHR (Figure 5) and BLM-induced dynamic lung compliance (Figure 7)

respectively. Mice subjected to OVA/NA had significantly increased AHR compared to that measured from healthy controls (Figure 5). This was unaffected by 5-µg exosomes alone but was partially (by ~50%) and significantly reduced by 25-µg exosomes alone, serelaxin alone, or AEC + serelaxin. Strikingly, the presence of serelaxin enhanced the

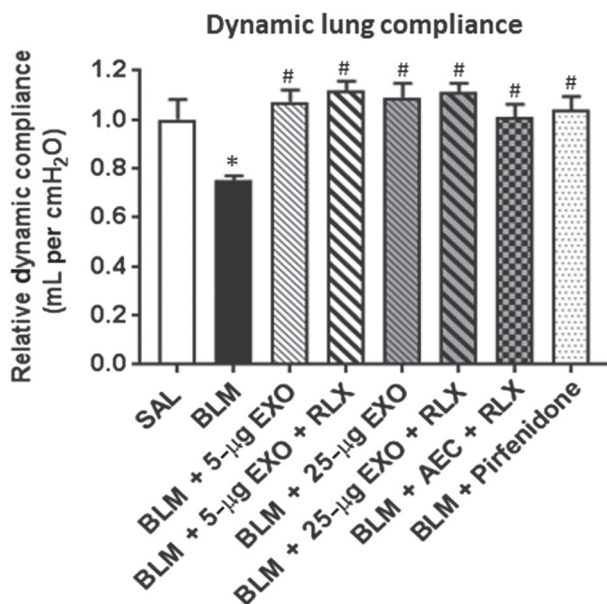


FIGURE 7 The effects of exosomes on BLM-induced dynamic lung compliance in the absence or presence of serelaxin. Shown is the relative mean \pm SEM dynamic lung compliance from control (saline), BLM-injured mice and from the various treatment groups investigated against BLM-induced pulmonary fibrosis, in response to the highest dose of methacholine evaluated ($50 \text{ mg}\cdot\text{ml}^{-1}$). * $P < 0.05$, significantly different from the control group (SAL); # $P < 0.05$, significantly different from the BLM-treated group

ability to 5- μg exosomes to reduce AHR by $\sim 70\%$ and the ability of 25- μg exosomes to reduce AHR to levels that were no longer different to that measured from SAL/CO control mice (Figure 5).

Mice subjected to BLM had a significant decrease ($\sim 25\%$) in dynamic lung compliance compared to that measured from controls (Figure 7). This was restored by all treatments investigated (Figure 7).

4 | DISCUSSION AND CONCLUSIONS

Several key findings were obtained from this study, which investigated the therapeutic potential of exosomes as a treatment for fibrotic lung disorders, with or without an anti-fibrotic agent, serelaxin. First, like their parental AECs (Royce et al., 2016; Tan et al., 2018), exosomes alone for the most part demonstrated partial anti-inflammatory, anti-remodelling, and anti-fibrotic protection against chronic AAD- and established BLM-induced lung injury/damage. As fibrosis can act as a barrier to stem cell survival, viability, migration, and integration with resident tissue cells (Eun et al., 2011; Lu et al., 2004), it is likely that established scar tissue can also impede the therapeutic effects of exosomes that are secreted by AECs. Interestingly, dose-dependent therapeutic effects of exosomes were observed in the model of OVA/NA-induced chronic AAD, but not in the model of BLM-induced pulmonary fibrosis (Tan et al., 2018), suggesting that administering increased doses of exosomes will not always provide added therapeutic benefits over that of lower doses. Although the distribution and therapeutic efficacy of injected exosomes within the animal body can vary

depending on their route of administration, on the cell type involved and the labelling system used (Wiklander et al., 2015), and it was unclear how many vesicles were present in the airways/lung post-administration until the time of tissue collection, our previous bioluminescence imaging studies demonstrated that intranasal administration of stem cells (that was used to administer AECs or exosomes into the lungs of OVA/NA- and BLM-injured mice in this study) delivered them directly into the lungs of mice (Royce et al., 2015). Therefore, it is more likely that the fibrosis associated with established organ injury, rather than the dose of exosomes administered or their ability to be delivered to the airways/lung, affected their therapeutic potential.

Second, this study demonstrated for the first time that co-administration of an anti-fibrotic and organ-protective drug, serelaxin (Bathgate et al., 2013; Samuel et al., 2017; Sarwar et al., 2017) was able to enhance some of the therapeutic effects of the exosomes. Combining exosomes with serelaxin resulted in greater anti-inflammatory, anti-remodelling, and anti-fibrotic effects, compared with either treatment alone and resulted in the normalization of OVA/NA-induced airway epithelial thickness and damage, subepithelial and total collagen deposition (fibrosis), myofibroblast differentiation and AHR; and BLM-induced lung inflammation, epithelial damage, interstitial TGF- $\beta 1$ expression, interstitial and subepithelial fibrosis, and dynamic compliance, after as little as a 7-day treatment period. Combining serelaxin with exosomes also rapidly reversed airway/lung epithelial thickness, damage and related fibrosis as well as lung dysfunction to an equivalent extent as the combined effects of serelaxin and 1×10^6 AECs, but more effectively reduced organ inflammation, several aspects of airway/lung remodelling and AHR compared to the combined effects of serelaxin and AECs; suggesting that co-administration of serelaxin and exosomes offered some level of improved tissue protection over that of combining serelaxin with AECs. Although the synergistic effects of serelaxin were less pronounced in the presence of the higher dose of exosomes (25 μg) used, most likely due to the improved or trend towards improved airway/lung protection offered by 25- μg exosomes over the 5- μg dose, the current study also confirmed that serelaxin pretreatment was not required to enhance the effects of exosomes.

These findings may be explained by a number of advantages to the use of exosomes as therapeutic agents. As exosomes are non-living entities, they can be frozen and thawed for immediate use, whereas AECs cannot be stored at -80°C for long periods and when thawed may be subject to the toxic effects of DMSO and several hours of preparation for therapeutic application (Murphy et al., 2014). In this study, the therapeutic effects of approximately 2.5 and 12.5 million AECs were administered in the form of 5 and 25 μg of exosomes, respectively, whereas only 1–2 million AECs can physically be administered to mice in a single dose. Therefore, the findings presented could simply be the result of the greater therapeutic effects of the exosomes administered (over that of the 1 million AECs that were used for comparison) and then combined with serelaxin. Combining exosomes with serelaxin could also have promoted synergistic actions through the activation of overlapping and distinct pathways. Serelaxin can inhibit the contribution of lung inflammation on fibrosis by reducing the infiltration and activation of

mast cells (Bani, Ballati, Masini, Bigazzi, & Sacchi, 1997), leukocytes (Bani et al., 1997; Pini, Boccalini, Lucarini, et al., 2016), and neutrophils (Masini et al., 2004) and suppressing the pro-inflammatory and pro-fibrotic actions of TGF- β 1 (Royce, Lim, et al., 2014; Unemori et al., 1996), TNF- α , IL-1 β , and/or IL-18 (Brecht, Bartsch, Baumann, Stangl, & Dschietzig, 2011; Pini, Boccalini, Baccari, et al., 2016). Furthermore, serelaxin inhibits fibrosis by preventing fibroblast proliferation and differentiation into myofibroblasts as a means of limiting myofibroblast-mediated ECM deposition (Huuskens et al., 2015; Royce et al., 2015, 2016).

On the other hand, exosomes have been implicated in regulating cytokine signalling associated with the innate immune system, **toll-like receptor** signalling, TGF- β 1-induced TNF receptor associated factor-6 and **MAPK** activity, and cell junction signalling (Tan et al., 2018). In particular, exosomes were found to reduce BLM-induced expression of **bone morphogenic protein 4** (a member of the TGF- β superfamily) and lymphoid enhancer binding factor 1 (which is involved in TGF- β 1/Wnt signalling; Tan et al., 2018). Exosomes also inhibited the migration and proliferation of fibroblasts and ECM deposition (Zhao et al., 2017). Additionally, exosomes contain microRNAs (such as miR-23a and miR-150) that can inhibit fibrosis (Tan et al., 2018). For example, studies conducted in mice have shown that over-expression of miR-23a in conjunction with miR-27a inhibited diabetes-induced TGF- β 1 signal transduction, myofibroblast differentiation, and related renal fibrosis (Zhang et al., 2018), while over-expression of miR-150 could inhibit cardiac fibroblast activation (into myofibroblasts) and related fibrosis (Deng et al., 2016).

Third, this study demonstrated that while exosomes alone were more effective in reducing interstitial (collagen I-related) lung fibrosis (Figure 4f), serelaxin administration was required to augment the effects of exosomes in also reducing BM/collagen IV-related fibrosis (Glasser et al., 2016); providing a net effect of more effectively reducing total collagen deposition and fibrosis. Interestingly, combining 25- μ g exosomes with serelaxin had a doubling effect over that of 25- μ g exosomes alone in reducing and normalizing OVA-NA-induced BM/subepithelial fibrosis (Figure 1e) and total lung concentration (Figure 1f), as well as BLM-induced BM/subepithelial fibrosis (Figure 3d). These findings suggest that serelaxin can enhance the ability of exosomes to treat BM/subepithelial remodelling and fibrosis, given that exosomes alone appeared to be more effective in treating interstitial remodelling and fibrosis, to reduce total lung fibrosis.

Fourth, the current findings build upon on our recent studies (Patel et al., 2016; Royce et al., 2015, 2016) in demonstrating that, while targeting airway fibrosis and epithelial damage (rather than airway inflammation) is key to effectively reducing AHR, that this alone may not be enough to fully protect from adverse changes in airway reactivity, and hence, targeting other measures of airway remodelling is required to fully reverse airway reactivity. This was highlighted by the fact that while the combined effects of serelaxin with either 25- μ g exosomes or 1×10^6 AECs were able to normalize OVA/NA-induced epithelial thickness and subepithelial and total collagen deposition, the combined effects of serelaxin and 25- μ g exosomes were also able to reduce OVA/NA-induced airway inflammation, goblet cell

metaplasia, epithelial TGF- β 1 expression and myofibroblast accumulation; and BLM-induced epithelial damage, interstitial TGF- β 1 expression, and myofibroblast accumulation to a greater extent than the combined effects of serelaxin and AECs. As a result, the combined effects of serelaxin and 25- μ g exosomes were able to normalize OVA/NA-induced AHR after 7 days, whereas the combined effects of serelaxin and AECs only partly reduced AHR, by ~50%.

Finally, the findings from the current study suggest that combining 25- μ g exosomes with serelaxin may represent a stand-alone means of treating the 5–10% of asthmatics that are resistant to corticosteroid therapy (Fleming, Wilson, & Bush, 2007; Hetherington & Heaney, 2015). As corticosteroids, a current anti-inflammatory asthma medication, can be slow acting and induce several side effects when chronically administered, particularly at high doses (Dahl, 2006), lower doses of corticosteroids may be combined with exosomes and serelaxin to treat the three central components of asthma without causing any of the side effects associated with higher concentrations of corticosteroid use alone. The same could be applied to pirfenidone for the treatment of pulmonary fibrosis, as pirfenidone primarily targets interstitial fibrosis (Figure 3b) and can also be associated with several side effects when therapeutically administered (Jiang et al., 2012). As AECs (Lim, Hodge, Moore, Wallace, & Sievert, 2017), exosomes (ClinicalTrials.gov Identifier NCT02138331; NCT03384433), and serelaxin (Teerlink et al., 2013) have separately been evaluated in clinical trials, novel strategies incorporating this combination therapy can be fast-tracked for human trials.

In conclusion, the present study demonstrates for the first time, the ability of the anti-fibrotic and organ-protective drug, serelaxin, to enhance some of the therapeutic effects of exosomes. Combining serelaxin with 25- μ g exosomes offered the broader protection from airway/lung inflammation, remodelling, fibrosis, and related dysfunction over the effects of each treatment alone, the combined effects of serelaxin and 1×10^6 AECs or pirfenidone. Particularly noteworthy was the finding that serelaxin augmented the ability of exosomes to reduce BM fibrosis, which contributed to a greater ability of the combination therapy to reduce overall fibrosis. Although further studies are warranted to evaluate the mechanisms by which this combination therapy mediates its tissue-protective effects and address some of the limitations of this study in that (a) the exact composition of the exosomes used was not fully characterized, (b) the migration of exosomes post-intranasal delivery was not tracked nor was it determined, and (c) how many exosomes were present in the airways/lung post-administration, our findings clearly demonstrated that the combined effects of serelaxin and exosomes may represent a novel and rapidly effective approach to treating fibrosis-related disorders which are significant health burdens and contributors to substantial morbidity and mortality.

ACKNOWLEDGEMENTS

This study was supported in part by a Monash University MBio Post-graduate Discovery Scholarship (MPDS) to K.P.P.; a National Health and Medical Research Council (NHMRC) of Australia Senior Research

Fellowships to C.S.S. (Grant GNT1041766); and Monash Innovation Research Funding to C.S.S. and R.L.

AUTHOR CONTRIBUTIONS

S.G.R. and C.S.S. participated in research design. S.G.R., K.P.P., W.M., D.Z., and C.S.S. conducted experiments. D.Z. and R.L. contributed reagents or tools. S.G.R., K.P.P., W.M., and C.S.S. performed data analysis. S.G.R., K.P.P., W.M., D.Z., R.L., and C.S.S. wrote or contributed to writing of manuscript.

CONFLICT OF INTEREST

The authors declare no conflicts of interest.

DECLARATION OF TRANSPARENCY AND SCIENTIFIC RIGOUR

This Declaration acknowledges that this paper adheres to the principles for transparent reporting and scientific rigour of preclinical research as stated in the *BJP* guidelines for [Design & Analysis](#), [Immunoblotting and Immunochemistry](#), and [Animal Experimentation](#), and as recommended by funding agencies, publishers and other organisations engaged with supporting research.

ORCID

Chrishan S. Samuel  <https://orcid.org/0000-0003-0295-4214>

REFERENCES

- Afratis, N. A., Selman, M., Pardo, A., & Sagi, I. (2018). Emerging insights into the role of matrix metalloproteases as therapeutic targets in fibrosis. *Matrix Biology*, 68–69, 167–179. <https://doi.org/10.1016/j.matbio.2018.02.007>
- Akle, C. A., Adinolfi, M., Welsh, K. I., Leibowitz, S., & McColl, I. (1981). Immunogenicity of human amniotic epithelial cells after transplantation into volunteers. *Lancet*, 2, 1003–1005.
- Alexander, S. P. H., Christopoulos, A., Davenport, A. P., Kelly, E., Marrion, N. V., Peters, J. A., ... CGTP Collaborators. (2017). The Concise Guide to PHARMACOLOGY 2017/18: G protein-coupled receptors. *British Journal of Pharmacology*, 174, S17–S129. <https://doi.org/10.1111/bph.13878>
- Alexander, S. P. H., Fabbro, D., Kelly, E., Marrion, N. V., Peters, J. A., Faccenda, E., ... CGTP Collaborators. (2017a). The Concise Guide to PHARMACOLOGY 2017/18: Catalytic receptors. *British Journal of Pharmacology*, 174, S225–S271. <https://doi.org/10.1111/bph.13876>
- Alexander, S. P. H., Fabbro, D., Kelly, E., Marrion, N. V., Peters, J. A., Faccenda, E., ... CGTP Collaborators. (2017b). The Concise Guide to PHARMACOLOGY 2017/18: Enzymes. *British Journal of Pharmacology*, 174, S272–S359. <https://doi.org/10.1111/bph.13877>
- Bani, D., Ballati, L., Masini, E., Bigazzi, M., & Sacchi, T. B. (1997). Relaxin counteracts asthma-like reaction induced by inhaled antigen in sensitized guinea pigs. *Endocrinology*, 138, 1909–1915. <https://doi.org/10.1210/endo.138.5.5147>
- Basu, J., & Ludlow, J. W. (2016). Exosomes for repair, regeneration and rejuvenation. *Expert Opin Biol Therap*, 16, 489–506. <https://doi.org/10.1517/14712598.2016.1131976>
- Bathgate, R. A., Halls, M. L., van der Westhuizen, E. T., Callander, G. E., Kocan, M., & Summers, R. J. (2013). Relaxin family peptides and their receptors. *Physiological Reviews*, 93, 405–480. <https://doi.org/10.1152/physrev.00001.2012>
- Brecht, A., Bartsch, C., Baumann, G., Stangl, K., & Dschietzig, T. (2011). Relaxin inhibits early steps in vascular inflammation. *Regulatory Peptides*, 166, 76–82. <https://doi.org/10.1016/j.regpep.2010.09.001>
- Dahl, R. (2006). Systemic side effects of inhaled corticosteroids in patients with asthma. *Respiratory Medicine*, 100, 1307–1317. <https://doi.org/10.1016/j.rmed.2005.11.020>
- Deng, P., Chen, L., Liu, Z., Ye, P., Wang, S., Wu, J., ... Chen, M. (2016). MicroRNA-150 inhibits the activation of cardiac fibroblasts by regulating c-Myb. *Cellular Physiology and Biochemistry*, 38, 2103–2122. <https://doi.org/10.1159/000445568>
- Eming, S. A., Wynn, T. A., & Martin, P. (2017). Inflammation and metabolism in tissue repair and regeneration. *Science*, 356, 1026–1030. <https://doi.org/10.1126/science.aam7928>
- Eun, L. Y., Song, H., Choi, E., Lee, T. G., Moon, D. W., Hwang, D., ... Hwang, K. C. (2011). Implanted bone marrow-derived mesenchymal stem cells fail to metabolically stabilize or recover electromechanical function in infarcted hearts. *Tissue & Cell*, 43, 238–245. <https://doi.org/10.1016/j.tice.2011.04.002>
- Fleming, L., Wilson, N., & Bush, A. (2007). Difficult to control asthma in children. *Current Opinion in Allergy and Clinical Immunology*, 7, 190–195. <https://doi.org/10.1097/ACI.0b013e3280895d0c>
- Gallop, P. M., & Paz, M. A. (1975). Posttranslational protein modifications, with special attention to collagen and elastin. *Physiological Reviews*, 55, 418–487. <https://doi.org/10.1152/physrev.1975.55.3.418>
- Glasser, S. W., Hagood, J. S., Wong, S., Taype, C. A., Madala, S. K., & Hardie, W. D. (2016). Mechanisms of lung fibrosis resolution. *Am J Path*, 186, 1066–1077. <https://doi.org/10.1016/j.ajpath.2016.01.018>
- Harding, S. D., Sharman, J. L., Faccenda, E., Southan, C., Pawson, A. J., Ireland, S., ... NC-IUPHAR. (2018). The IUPHAR/BPS Guide to PHARMACOLOGY in 2018: updates and expansion to encompass the new guide to IMMUNOPHARMACOLOGY. *Nucleic Acids Res*, 46, D1091–D1106. <https://doi.org/10.1093/nar/gkx1121>
- Hetherington, K. J., & Heaney, L. G. (2015). Drug therapies in severe asthma –The era of stratified medicine. *Clinical Medicine (London, England)*, 15, 452–456. <https://doi.org/10.7861/clinmedicine.15-5-452>
- Huuskens, B. M., Wise, A. F., Cox, A. J., Lim, E. X., Payne, N. L., Kelly, D. J., ... Ricardo, S. D. (2015). Combination therapy of mesenchymal stem cells and serelaxin effectively attenuates renal fibrosis in obstructive nephropathy. *The FASEB Journal*, 29, 540–553. <https://doi.org/10.1096/fj.14-254789>
- Jiang, C., Huang, H., Liu, J., Wang, Y., Lu, Z., & Xu, Z. (2012). Adverse events of pirfenidone for the treatment of pulmonary fibrosis: A meta-analysis of randomized controlled trials. *PLoS ONE*, 7, e47024. <https://doi.org/10.1371/journal.pone.0047024>
- Kilkenny, C., Browne, W., Cuthill, I. C., Emerson, M., & Altman, D. G. (2010). Animal research: Reporting in vivo experiments: The ARRIVE guidelines. *British Journal of Pharmacology*, 160, 1577–1579.
- Kumar, R. K., Herbert, C., & Foster, P. S. (2008). The “classical” ovalbumin challenge model of asthma in mice. *Current Drug Targets*, 9, 485–494. <https://doi.org/10.2174/138945008784533561>
- Lim, R., Hodge, A., Moore, G., Wallace, E. M., & Sievert, W. (2017). A pilot study evaluating the safety of intravenously administered human amnion epithelial cells for the treatment of hepatic fibrosis. *Frontiers in Pharmacology*, 8, 549. <https://doi.org/10.3389/fphar.2017.00549>
- Lu, L., Zhang, J. Q., Ramires, F. J., & Sun, Y. (2004). Molecular and cellular events at the site of myocardial infarction: From the perspective of rebuilding myocardial tissue. *Biochemical and Biophysical Research*

- Communications, 320, 907–913. <https://doi.org/10.1016/j.bbrc.2004.06.034>
- Masini, E., Nistri, S., Vannacci, A., Bani Sacchi, T., Novelli, A., & Bani, D. (2004). Relaxin inhibits the activation of human neutrophils: Involvement of the nitric oxide pathway. *Endocrinology*, 145, 1106–1112. <https://doi.org/10.1210/en.2003-0833>
- Miki, T., Lehmann, T., Cai, H., Stolz, D. B., & Strom, S. C. (2005). Stem cell characteristics of amniotic epithelial cells. *Stem Cells*, 23, 1549–1559. <https://doi.org/10.1634/stemcells.2004-0357>
- Moeller, A., Ask, K., Warburton, D., Gaudie, J., & Kolb, M. (2008). The bleomycin animal model: A useful tool to investigate treatment options for idiopathic pulmonary fibrosis? *The International Journal of Biochemistry & Cell Biology*, 40, 362–382. <https://doi.org/10.1016/j.biocel.2007.08.011>
- Molnar, C., & Gain, J. (2012). Section 12.2: Innate immunity. In *Concepts of biology-1st Canadian edition*. Houston, Texas: OpenStax College (Rice University).
- Moodley, Y., Ilancheran, S., Samuel, C., Vaghjiani, V., Atienza, D., Williams, E. D., ... Manuelpillai, U. (2010). Human amnion epithelial cell transplantation abrogates lung fibrosis and augments repair. *American Journal of Respiratory and Critical Care Medicine*, 182, 643–651. <https://doi.org/10.1164/rccm.201001-0014OC>
- Murphy, S., Rosli, S., Acharya, R., Mathias, L., Lim, R., Wallace, E., & Jenkin, G. (2010). Amnion epithelial cell isolation and characterization for clinical use. *Current Protocols in Stem Cell Biology*. Chapter 1: Unit, 1E, 6.
- Murphy, S. V., Kidoor, A., Reid, T., Atala, A., Wallace, E. M., & Lim, R. (2014). Isolation, cryopreservation and culture of human amnion epithelial cells for clinical applications. *Journal of Visualized Experiments*, 2014(94).
- Oku, H., Shimizu, T., Kawabata, T., Nagira, M., Hikita, I., Ueyama, A., ... Arimura, A. (2008). Antifibrotic action of pirfenidone and prednisolone: Different effects on pulmonary cytokines and growth factors in bleomycin-induced murine pulmonary fibrosis. *European Journal of Pharmacology*, 590, 400–408. <https://doi.org/10.1016/j.ejphar.2008.06.046>
- Patel, K. P., Giraud, A. S., Samuel, C. S., & Royce, S. G. (2016). Combining an epithelial repair factor and anti-fibrotic with a corticosteroid offers optimal treatment for allergic airways disease. *British Journal of Pharmacology*, 173, 2016–2029. <https://doi.org/10.1111/bph.13494>
- Pini, A., Boccalini, G., Baccari, M. C., Becatti, M., Garella, R., Fiorillo, C., ... Nistri, S. (2016). Protection from cigarette smoke-induced vascular injury by recombinant human relaxin-2 (serelaxin). *Journal of Cellular and Molecular Medicine*, 20, 891–902. <https://doi.org/10.1111/jcmm.12802>
- Pini, A., Boccalini, G., Lucarini, L., Catarinicchia, S., Guasti, D., Masini, E., ... Nistri, S. (2016). Protection from cigarette smoke-induced lung dysfunction and damage by H2 relaxin (serelaxin). *Journal of Pharmacology and Experimental Therapeutics*, 357, 451–458. <https://doi.org/10.1124/jpet.116.232215>
- Royce, S. G., Lim, C. X., Patel, K. P., Wang, B., Samuel, C. S., & Tang, M. L. (2014). Intranasally administered serelaxin abrogates airway remodeling and attenuates airway hyperresponsiveness in allergic airways disease. *Clinical and Experimental Allergy*, 44, 1399–1408. <https://doi.org/10.1111/cea.12391>
- Royce, S. G., Moodley, Y., & Samuel, C. S. (2014). Novel therapeutic strategies for lung disorders associated with airway remodelling and fibrosis. *Pharmacology & Therapeutics*, 141, 250–260. <https://doi.org/10.1016/j.pharmthera.2013.10.008>
- Royce, S. G., Patel, K. P., & Samuel, C. S. (2014). Characterization of a novel model incorporating airway epithelial damage and related fibrosis to the pathogenesis of asthma. *Laboratory Investigation*, 94, 1326–1339. <https://doi.org/10.1038/labinvest.2014.119>
- Royce, S. G., Shen, M., Patel, K. P., Huuskens, B. M., Ricardo, S. D., & Samuel, C. S. (2015). Mesenchymal stem cells and serelaxin synergistically abrogate established airway fibrosis in an experimental model of chronic allergic airways disease. *Stem Cell Research*, 15, 495–505. <https://doi.org/10.1016/j.scr.2015.09.007>
- Royce, S. G., Tominaga, A. M., Shen, M., Patel, K. P., Huuskens, B. M., Lim, R., ... Samuel, C. S. (2016). Serelaxin improves the therapeutic efficacy of RXFP1-expressing human amnion epithelial cells in experimental allergic airway disease. *Clinical Science (London, England)*, 130, 2151–2165. <https://doi.org/10.1042/CS20160328>
- Samuel, C. S., Royce, S. G., Hewitson, T. D., Denton, K. M., Cooney, T. E., & Bennett, R. G. (2017). Anti-fibrotic actions of relaxin. *British Journal of Pharmacology*, 174, 962–976.
- Sarwar, M., Du, X. J., Dschietzig, T. B., & Summers, R. J. (2017). The actions of relaxin on the human cardiovascular system. *British Journal of Pharmacology*, 174, 933–949. <https://doi.org/10.1111/bph.13523>
- Tan, J. L., Lau, S. N., Leaw, B., Nguyen, H. P. T., Salamonsen, L. A., Saad, M. I., ... Lim, R. (2018). Amnion epithelial cell-derived exosomes restrict lung injury and enhance endogenous lung repair. *Stem Cells Translational Medicine*, 7, 180–196. <https://doi.org/10.1002/sctm.17-0185>
- Teerlink, J. R., Cotter, G., Davison, B. A., Felker, G. M., Filippatos, G., Greenberg, B. H., ... Metra, M. (2013). Serelaxin, recombinant human relaxin-2, for treatment of acute heart failure (RELAX-AHF): A randomised, placebo-controlled trial. *Lancet*, 381, 29–39. [https://doi.org/10.1016/S0140-6736\(12\)61855-8](https://doi.org/10.1016/S0140-6736(12)61855-8)
- Unemori, E. N., Pickford, L. B., Salles, A. L., Piercy, C. E., Grove, B. H., Erikson, M. E., & Amento, E. P. (1996). Relaxin induces an extracellular matrix-degrading phenotype in human lung fibroblasts in vitro and inhibits lung fibrosis in a murine model in vivo. *The Journal of Clinical Investigation*, 98, 2739–2745. <https://doi.org/10.1172/JCI119099>
- Wiklander, O. P., Nordin, J. Z., O'Loughlin, A., Gustafsson, Y., Corso, G., Mager, I., ... Andaloussi, S. E. (2015). Extracellular vesicle in vivo biodistribution is determined by cell source, route of administration and targeting. *Journal of Extracellular Vesicles*, 4, 26316. <https://doi.org/10.3402/jev.v4.26316>
- Wynn, T. A., & Ramalingam, T. R. (2012). Mechanisms of fibrosis: Therapeutic translation for fibrotic disease. *Nature Medicine*, 18, 1028–1040. <https://doi.org/10.1038/nm.2807>
- Zhang, A., Li, M., Wang, B., Klein, J. D., Price, S. R., & Wang, X. H. (2018). miRNA-23a/27a attenuates muscle atrophy and renal fibrosis through muscle-kidney crosstalk. *Journal of Cachexia, Sarcopenia and Muscle*, 9, 755–770. <https://doi.org/10.1002/jcsm.12296>
- Zhao, B., Zhang, Y., Han, S., Zhang, W., Zhou, Q., Guan, H., ... Hu, D. (2017). Exosomes derived from human amniotic epithelial cells accelerate wound healing and inhibit scar formation. *Journal of Molecular Histology*, 48, 121–132. <https://doi.org/10.1007/s10735-017-9711-x>

How to cite this article: Royce SG, Patel KP, Mao W, Zhu D, Lim R, Samuel CS. Serelaxin enhances the therapeutic effects of human amnion epithelial cell-derived exosomes in experimental models of lung disease. *Br J Pharmacol*. 2019;176: 2195–2208. <https://doi.org/10.1111/bph.14666>